JOURNAL OF SOLID STATE CHEMISTRY 58, 233–242 (1985)

Formation of Pentagonal Tunnels Bordered with P_2O_7 Groups in Diphosphate Tungsten Bronzes $(P_2O_4)_2(WO_3)_{2m}$: A HREM Investigation

MARYVONNE HERVIEU, BERNADETTE DOMENGÈS, AND BERNARD RAVEAU

Laboratoire de Cristallographie, Chimie et Physique des Solides, L.A. 251, ISMRA—Université, 14032 Caen Cédex, France

Received July 30, 1984; in revised form December 3, 1984

During the investigation of the phosphate bronzes $(PO_2)_4(WO_3)_{2m}$ [$MPTB_P$] and $K_x(P_2O_4)_2(WO_3)_{2m}$ [$DPTB_H$] crystals of a new type were observed. HREM images of these crystals showed twinned ReO_3-type slabs the junction of which was parallel to the $(102)_{ReO_3}$ plane. The proposed model identified the twin boundary as built from P_2O_7 groups involving the formation of pentagonal tunnels. The structure of this new type of extended defects is quite original: it corresponds to a new structural type named "diphosphate tungsten bronzes with pentagonal tunnels" [$DPTB_P$], for which no regular member could be synthesized. Image calculations were performed to confirm the junction model. Apart from the disordered stacking of the ReO_3-type slabs, very few defects were observed and shear planes were only obtained in reduced samples. This new structural type takes its place in the large family of phosphate tungsten bronzes where all members ($DPTB_H$, $MPTB_H$, $MPTB_P$) are very closely related.

The recent investigation of the systems P–W–O and *A*–P–W–O (*A* = K, Rb, Tl, Ba) has shown the existence of a large family of phosphate tungsten bronzes, PTB (*1–9*). Three structural series of bronzes, built up from ReO_3-type slabs, were isolated: the diphosphate tungsten bronzes, $DPTB_H$, with hexagonal tunnels $A_x(P_2O_4)_2(WO_3)_{2m}$ (*A* = K, Rb, Tl, Ba), the monophosphate tungsten bronzes $MPTB_P$, with pentagonal tunnels $(PO_2)_4(WO_3)_{2m}$, and the monophosphate tungsten bronzes, $MPTB_H$, with hexagonal tunnels $A_x(PO_2)_4(WO_3)_{2m}$ (*A* = Na, K).

An analysis of the structural relationships among these three series let us think of the possibility of formation of diphosphate tungsten bronzes with pentagonal tunnels. However, no phase corresponding to this structure was observed in the $A_x(P_2O_4)_2(WO_3)_{2m}$ oxides. This paper deals with the study of such a structure, which appeared as an almost regular sequence of "bi-dimensional" defects in a ReO_3-type matrix, during the investigation of the phosphate tungsten bronzes $(PO_2)_4(WO_3)_{2m}$ and $K_x(P_2O_4)_2(WO_3)_{2m}$.

Experimental

The synthesis of the phosphate tungsten bronzes $(PO_2)_4(WO_3)_{2m}$ and $K_x(P_2O_4)_2(WO_3)_{2m}$ by solid-state reaction in silica am-

0022-4596/85 $3.00

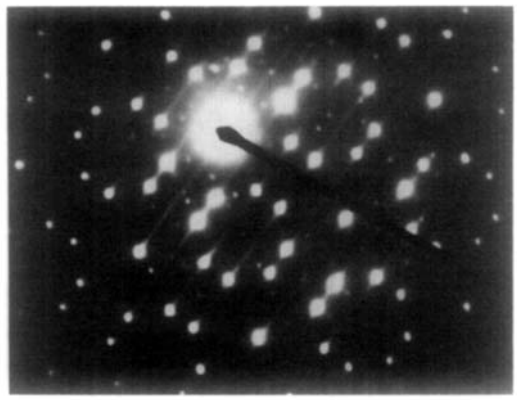

a

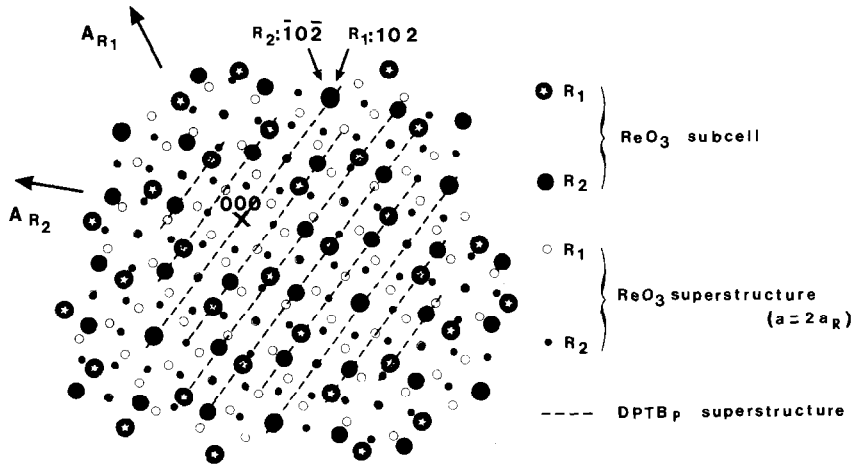

b

FIG. 1. (a) A typical (010) electron diffraction pattern of observed crystals. (b) Its schematic representation shows the twinned WO_3 areas.

poules has been previously described (*1–9*). Most of the crystals were very regular and characterized either by a $MPTB_P$ or a $DPTB_H$ structure. Some crystals exhibited different HREM micrographs, with a semiregular sequence; they were mostly observed for two nominal compositions: $(PO_2)_4(WO_3)_{36}$ and $K(P_2O_4)_2(WO_3)_{75}$.

To obtain HREM images, crystals were crushed in an agate mortar and dispersed in *n*-butanol. They were collected on holey carbon films supported by copper grids. Samples were examined in a Jeol 100 CX microscope, operating at 120 kV and equipped with a top-entry goniometer (±10°) and a lens with a spherical aberration constant C_s = 0.7 mm. Electron diffraction patterns were used for a precise alignment of the crystals along the short crystallographic *b* axis. The lattice images were computed by use of the multislice method [Skarnulis (10)].

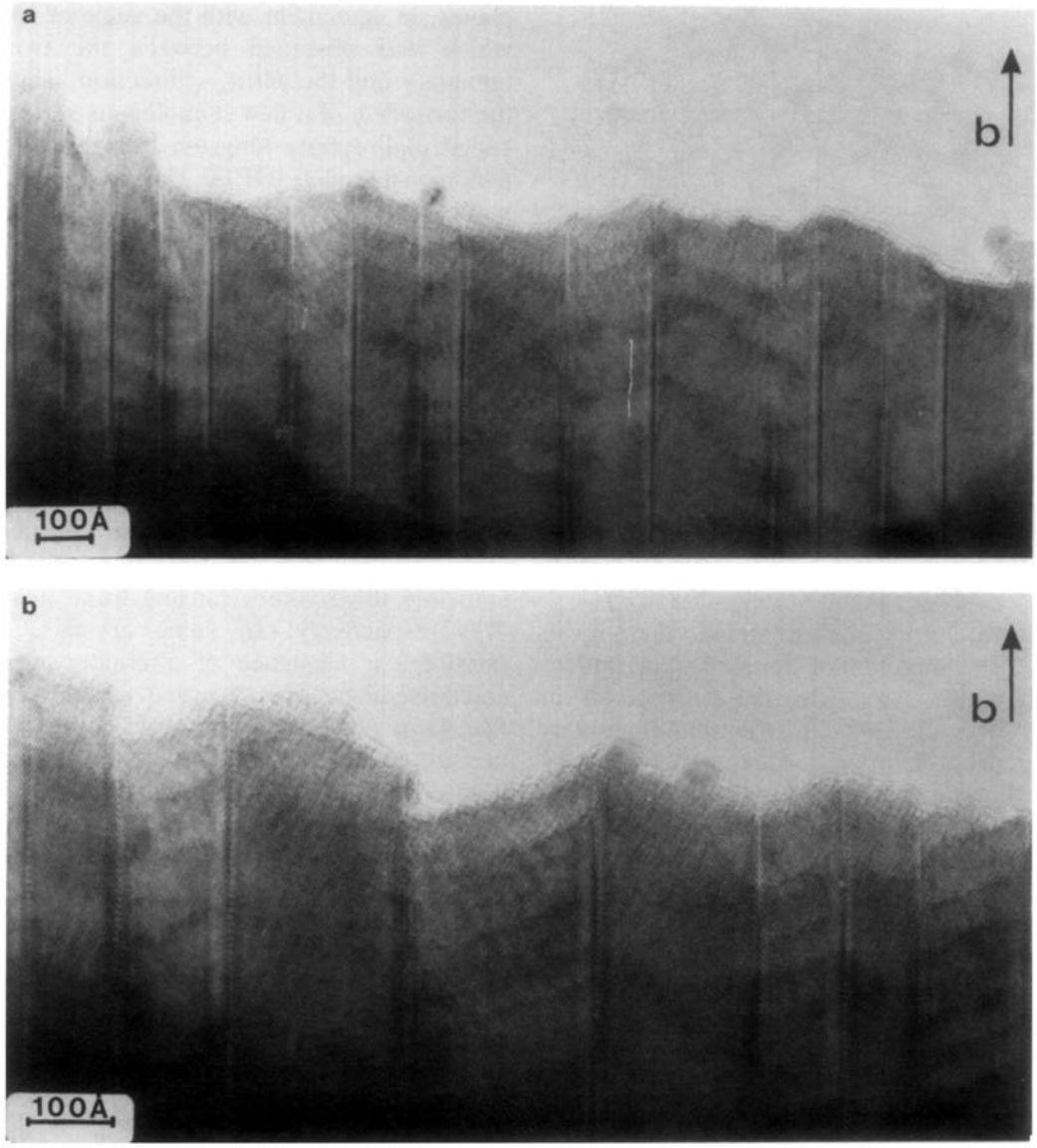

FIG. 2. High-resolution images projected down (010). (a) Twin domains of various width are observed. (b) Enlargement of a micrograph showing the WO_3 structure of each domain. The latter are inclined of 65° with respect to the twin boundary which appears as large white dots.

Results and Discussion

A New kind of Junction between ReO_3-type Slabs: "Diphosphate Planes" Form Pentagonal Tunnels

The "abnormal" crystals always exhibit the same electron diffraction pattern (Fig. 1a). The strongest reflections indicate the presence of a WO_3 substructure and are characteristic of twinned areas. Both sublattices of the electron diffraction pattern are indexed in Fig. 1b. Two types of weak spots are observed. The first corresponds to weak but well-defined spots which reveal a doubling of the a_R and c_R parameters of the WO_3-type cell ($a \sim c \sim 2 \times 3.8$ Å). The

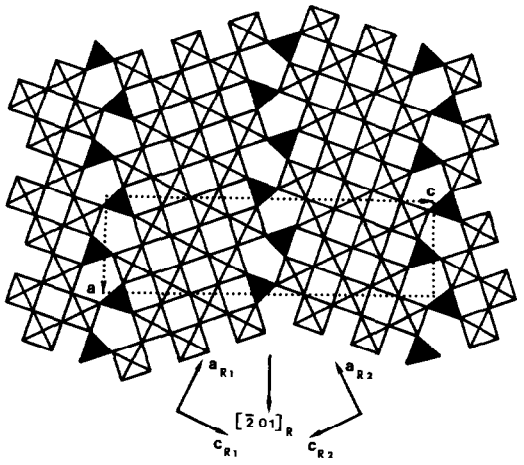

FIG. 3. Idealized projection onto (010) of the member $m = 7$ of the $(P_2O_4)_2$ $(WO_3)_{2m}$ structure type. The twin boundary consists of empty pentagonal tunnels.

second corresponds to streaks lined up in the |102| direction of the ReO_3-type lattice. They are similar to those observed in $DPTB_HS$ and {102} CS structures characterized by a disordered stacking of WO_3 slabs with various widths (*5, 11–14*). HREM micrographs of such crystals obtained with the *b* axis parallel to the electron beam are shown in Fig. 2. A sequence of "twin domains" can be observed. Each domain is formed of small white spots, regularly spaced (about 3.8 Å) along two perpendicular directions, which correspond to ReO_3-type tunnels. The twin boundary exhibits larger dots and is inclined 65° with respect to the |001| direction of the ReO_3-type domains.

If one considers that the larger dots, observed at the twin boundaries correspond to pentagonal tunnels, a model corresponding to a new structure can be proposed (Fig. 3). The framework of such a bronze would consist of ReO_3-type slabs connected through P_2O_7 groups by corner-sharing as in the $DPTB_HS$, but two P_2O_7 groups and three WO_6 octahedra would delimit pentagonal tunnels. In this model the pentagonal tunnels would also be located in the $(102)_{ReO_3}$ planes, in agreement with the angle of 65° which was observed between the twin boundary and the $|001|_{ReO_3}$ direction. Thus the formation of a new homologous series, called diphosphate tungsten bronzes with pentagonal tunnels ($DPTB_P$) is easily imaginable; the different members of this series $(P_2O_4)_2(WO_3)_{2m}$ would be characterized by an orthorhombic cell with the following parameters: $a \sim a_{ReO_3}\sqrt{5}$; $b \sim 2a_{ReO_3}$; and $c \sim 2m(a_{ReO_3}/\sqrt{5}) + 2K$ with $K \simeq 2.6$ Å. From the HREM observations, it is obvious that no regular member corresponding to this series could be synthesized. Nevertheless, it appears that semiregular sequences were observed, which involve such diphosphate planes. The boundary spacing can vary in a wide domain, from 46 to 720 Å, corresponding to *m* values ranging from 26 to 422, respectively. In some crystals, a quasiregular sequence of alternate small and large members is observed, as shown in Fig. 4a in which the mean observed *m* values are 48 and 91, respectively; but a random distribution of the ReO_3-type slabs is often observed (Fig. 4b).

In order to confirm this model of junction, synthetic HREM images were calculated, using the ideal structure of the member $m = 7$. The structure was assumed to be centrosymmetric; all the W atoms were supposed to be in one plane at $y = 0.25$ and in the center of regular octahedra. Calculations were carried out using the multislice method and programs FCOEFF and DEFECT written by Skarnulis (*10*). Through-focal series were calculated for different crystal thicknesses using the parameters: spherical aberration $C_s = 0.7$ mm; depth of focus = 170 Å; and incident beam convergence = 1.2 mrad. Figure 5 shows the calculated images with various defocus values for a crystal thickness of 22.8 Å.

The comparison of these calculated images, for a defocus value of −400 Å, with the enlarged lattice images (Fig. 6) confirms

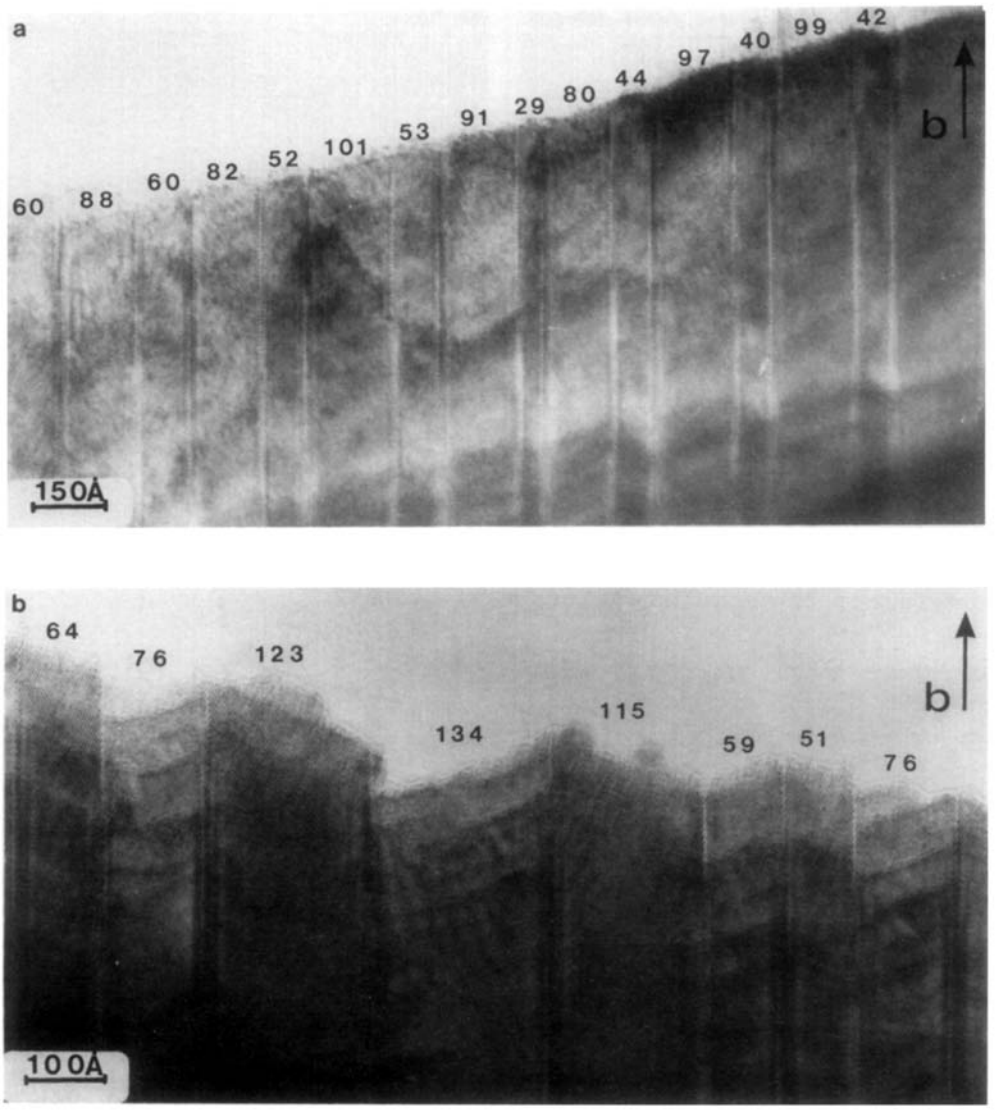

FIG. 4. $(P_2O_4)_2(WO_3)_{2m}$ micrographs projected down to (010). (a) Low-resolution image showing a quite regular distribution of alternate WO_3-slab widths in the mean sequence |48.91|. (b) High-resolution image showing a random stacking of WO_3 slabs.

that the junction of the ReO_3-type slabs consists of pentagonal tunnels running along **b**.

Possibility of Formation of Defects in the Disordered DPTB$_P$s

Contrary to the DPTB$_H$s, the disordered DPTB$_P$s do not exhibit many defects in spite of the irregular spacing of the diphosphate planes. It must be pointed out that the stopping of phosphate planes was never observed in the DPTB$_P$s. In the same way, no intergrowth of DPTB$_H$s and DPTB$_P$s could be observed, in spite of the similarity of the two structures.

In some crystals, defects leading to a

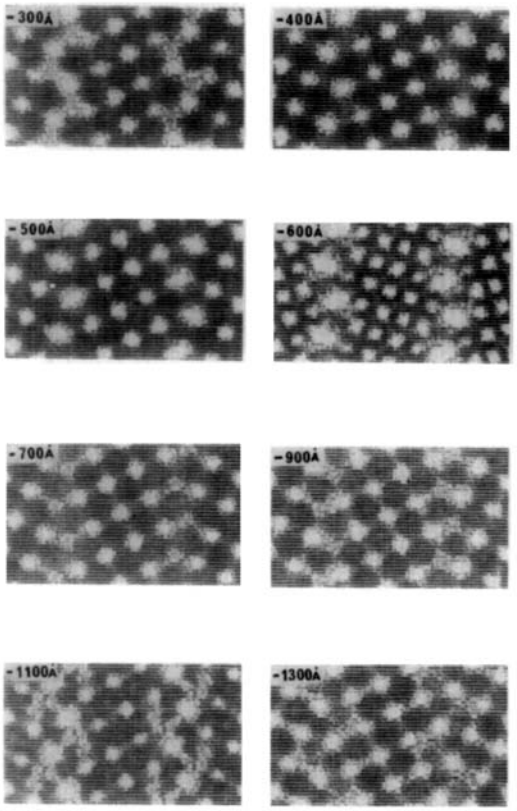

FIG. 5. Calculated through-focus images of the $(P_2O_4)_2(WO_3)_{14}$ structure (Δf = −300, −400, −500, −600, −700, −900, −1100, −1300 Å; t = 22.8 Å).

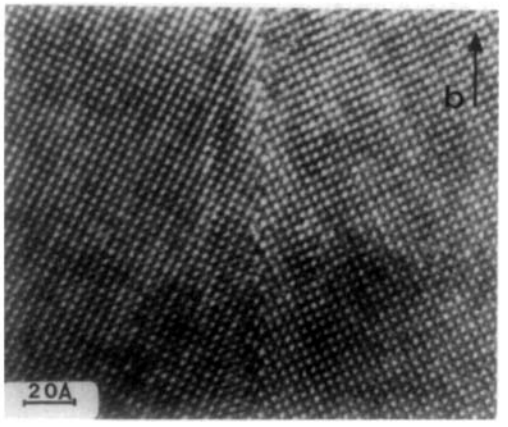

FIG. 6. High-resolution micrograph projected down to (010) of the twin boundary in a $(P_2O_4)_2(WO_3)_{2m}$ crystal. Its fitness with the calculated image for a −400-Å defocus value confirms the structural hypothesis.

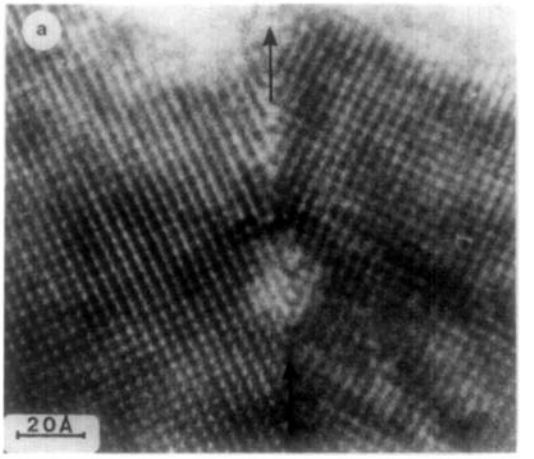

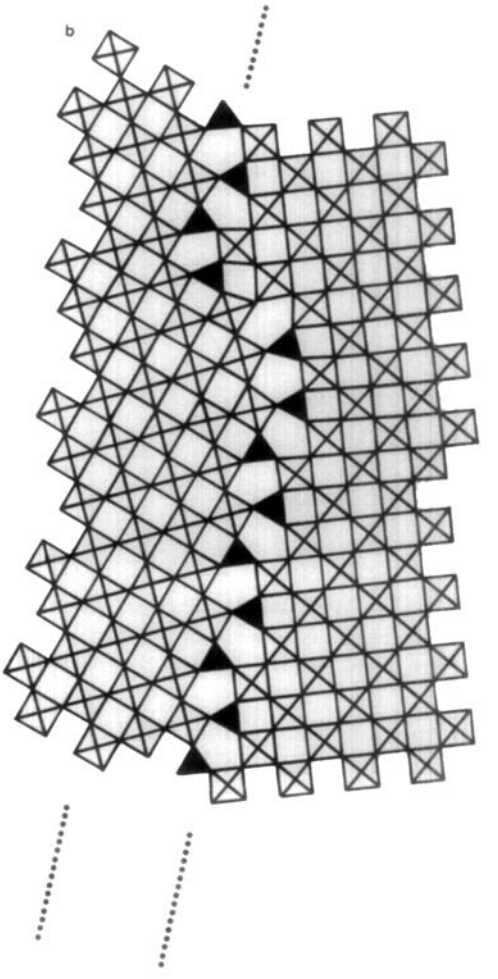

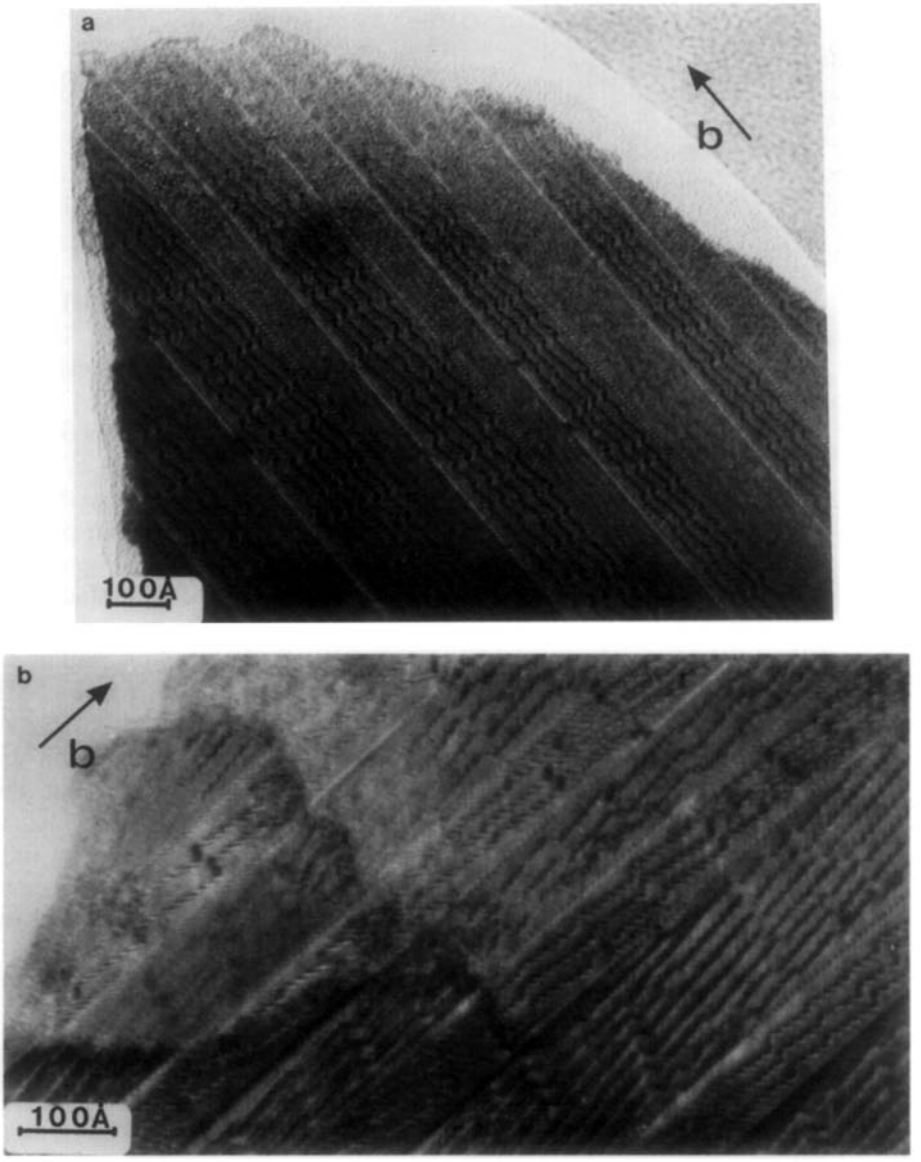

FIG. 8. High-resolution images of reduced $(P_2O_4)_2(WO_3)_{2m}$ crystals. (a) *CS* planes appear in wider WO_3 slabs. (b) Mixed {103} {001} *CS* planes are observed.

great perturbation of the matrix were observed (Fig. 7a). This type of defect corresponds to a shifting of the phosphate plane; it can be explained by a translation of the tunnel row of two octahedra along $|100|_{ReO_3}$ as shown from the idealized model proposed in Fig. 7b.

The formation of crystallographic shear

FIG. 7. Defect observed in a $(P_2O_4)_2(WO_3)_{2m}$ crystal. (a) High-resolution micrograph showing a shifting of the twin boundary. (b) Idealized model showing a two-octahedron translation of the tunnel row.

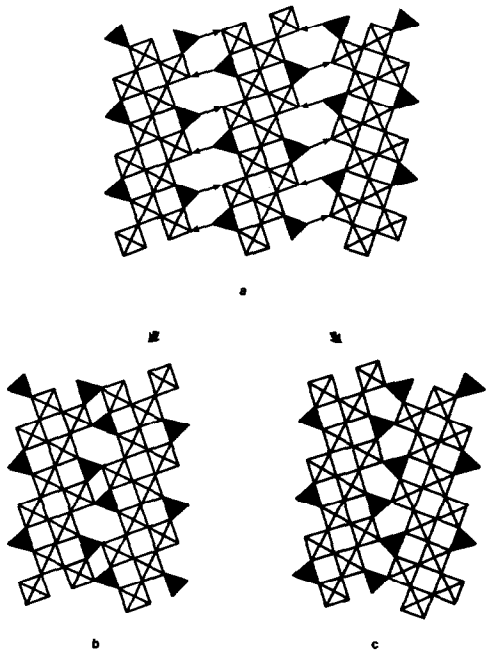

FIG. 9. Projection of mixed P_2O_7–WO_6 slabs L_D (a) the junction of which leads to the formation of either the $DPTB_H$ (b) or the $DPTB_P$ (c) structure type.

planes is not so easy as in $DPTB_HS$; $A_x(P_2O_4)_2(WO_3)_{2m}$ with A = K, Rb (*4*). No *CS* plane was observed in samples heated in evacuated silica ampoules. However, the heating of these samples in a reducing atmosphere (600°C, 2 hr, in the presence of zirconium in an evacuated silica ampoule) led to the formation of *CS* planes in the WO_3 slabs. As with the $DPTB_HS$, two sorts of *CS* planes were observed according to the width of the WO_3 slab (*4*): a single {102} *CS* plane and mixed {103}/{001} *CS* planes (Fig. 8).

Structural Relationships

This new type of connection is of interest in the study of the structural relationships in the phosphate tungsten bronzes. The $DPTB_HS$ and $DPTB_PS$ are built up from identical layers L_D of *m* octahedra bordered with P_2O_7 groups (Fig. 9a). The $DPTB_PS$ (Fig. 9c) are easily deduced from the $DPTB_HS$ (Fig. 9b) by 180° rotation of one of two layers around the *a* axis. This structural relationship is very similar to that observed for the monophosphate tungsten bronzes (*6*), which exhibit similar octahedral layers (L_M) but bordered with single PO_4 tetrahedra (Fig. 10a): the passage of the $MPTB_HS$ (Fig. 10b) to the $MPTB_PS$ (Fig. 10c) is absolutely identical, i.e., corresponds to the 180° rotation of one of the two layers.

The $DPTB_PS$ can be described in another way, namely as a packing of layers L_P formed of octahedra and single PO_4 tetrahedra, and parallel to the mean plane of the pentagonal ring (Fig. 11a). The structure of the $DPTB_PS$ results from the stacking of one layer L_P with one identical layer but deduced from L_P by a 180° rotation along **a** and **a**/2 translation. The $MPTB_PS$ $(PO_2)_4(WO_3)_{2m}$ (*1*) present closely related layers L'_P. The L'_P layers are built up from identical polyhedra with similar linkages but are in fact strongly corrugated due to the bent shape of the pentagonal ring (Fig. 11c). These L'_P layers are stacked up by corner-sharing their polyhedra so that two tet-

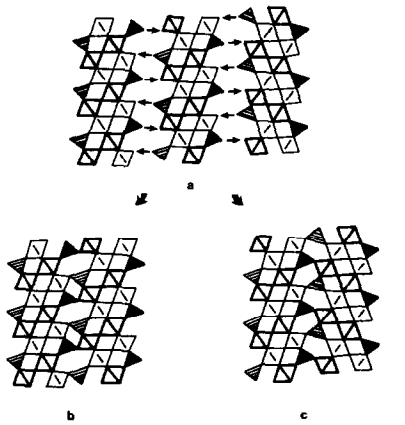

FIG. 10. Projection of mixed PO_4–WO_6 slabs L_M (a) the junction of which leads to the formation of either the $MPTB_H$ (b) or the $MPTB_P$ (c) structure type.

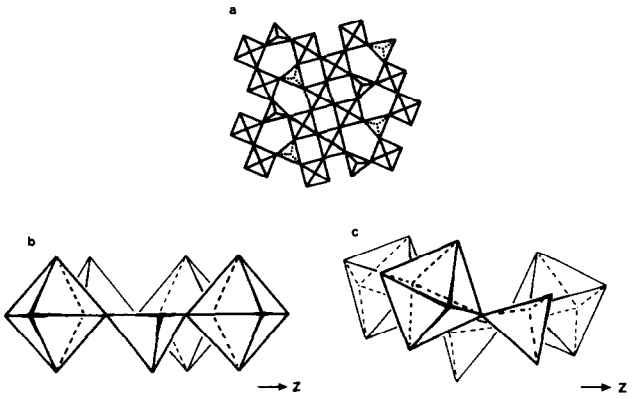

FIG. 11. (a) Projection onto (010) of a mixed PO_4–WO_6 layer L_p. (b) Projection parallel to the pentagonal ring of the latter in a layer L_p, stacking of which leads to the formation of the $DPTB_p$ structure type. (c) Projection parallel to the pentagonal ring of the latter in a corrugated layer L'_p stacking of which leads to the formation of the MPTBp structure type.

rahedra belonging to two different layers are never connected. Thus, it appears that the relationship between the $DPTB_p$s and $MPTB_p$s is very similar to that previously described between $DPTB_H$s and $MPTB_H$s (*2*), which involves L_H layers.

The structural mechanisms which characterize the formation of the different

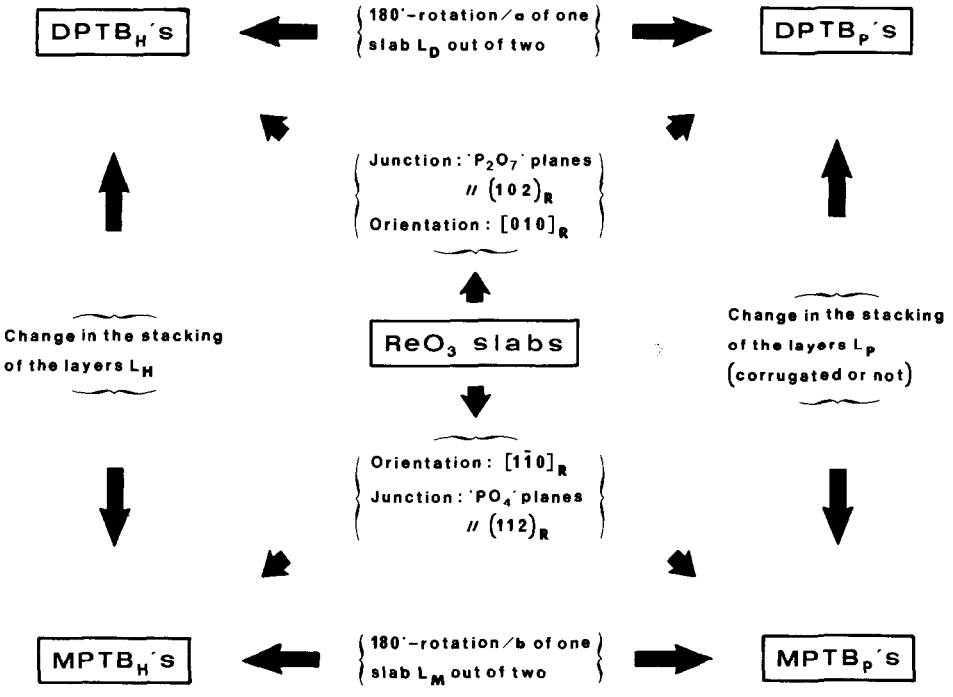

FIG. 12. Synoptic diagram of the phosphate tungsten bronzes.

frameworks of the phosphate tungsten bronzes, using a WO_3 matrix and phosphate groups, are summarized in Fig. 12. It appears that the relationships can easily be described by using $L_D(L_M)$, $L_p(L'_p)$, and $L_H(L'_H)$ layers.

The junction formed in the $DPTB_ps$ shows great similarity to that observed by Iijima (*15*) for ReO_3-orientated domains. The boundary of the latter is indeed parallel to $\{102\}_{ReO_3}$ and also forms pentagonal tunnels. It differs from that observed here by the absence of PO_4 tetrahedra and consists of interpenetrating TTB elements.

References

1. J. P. GIROULT, M. GOREAUD, PH. LABBÉ, AND B. RAVEAU, *Acta Crystallogr. B* **36,** 2570 (1980), **37,** 1163 (1981); **38,** 2139 (1982); **38,** 2342 (1982).
2. J. P. GIROULT, M. GOREAUD, PH. LABBÉ, AND B. RAVEAU, *J. Solid State Chem.* **44,** 407 (1982).
3. A. BENMOUSSA, PH. LABBÉ, D. GROULT, AND B. RAVEAU, *J. Solid State Chem.* **44,** 318 (1982).
4. M. HERVIEU AND B. RAVEAU, *Chem. Scr.* **22,** 117 (1983); **22,** 123 (1983).
5. M. HERVIEU AND B. RAVEAU, *J. Solid State Chem.* **44,** 299 (1982).
6. B. DOMENGÈS, M. GOREAUD, PH. LABBÉ, AND B. RAVEAU, *J. Solid State Chem.* **50,** 173 (1983).
7. B. DOMENGÈS, M. HERVIEU, AND B. RAVEAU, *Acta Crystallogr. B* **40,** 249 (1984).
8. B. DOMENGÈS, M. HERVIEU, R. J. D. TILLEY, AND B. RAVEAU, *J. Solid State Chem.* **54,** 10 (1984).
9. A. BENMOUSSA, D. GROULT, PH. LABBÉ, AND B. RAVEAU, *Acta Crystallogr. C* **40,** 573 (1984).
10. A. J. SKARNULIS, E. SUMMERVILLE, AND L. EYRING, *J. Solid State Chem.* **23,** 59 (1978).
11. S. IIJIMA, *J. Solid State Chem.* **14,** 52 (1975).
12. J. G. ALLPRESS, R. J. D. TILLEY, AND M. J. SIENKO, *J. Solid State Chem.* **3,** 440 (1971).
13. M. SUNDBERG, *J. Solid State Chem.* **35,** 120 (1980).
14. R. J. D. TILLEY, *Chem. Scr.* **14,** 147 (1979).
15. S. IIJIMA AND J. G. ALLPRESS, *Acta Crystallogr. A* **30,** 29 (1974).